

Switching Atomic Friction by Electrochemical Oxidation

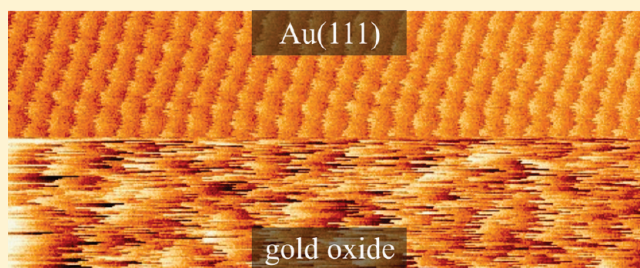
Aleksander Labuda,[†] Florian Hausen,[‡] Nitya Nand Gosvami,[‡] Peter H. Grütter,[†] R. Bruce Lennox,[§] and Roland Bennewitz^{*,‡}

[†]Department of Physics, McGill University, Montreal, Canada

[‡]INM - Leibniz Institute for New Materials, Saarbrücken, Germany

[§]Department of Chemistry, McGill University, Montreal, Canada

ABSTRACT: Friction between the sliding tip of an atomic force microscope and a gold surface changes dramatically upon electrochemical oxidation of the gold surface. Atomic-scale variations of the lateral force reveal details of the friction mechanisms. Stick–slip motion with atomic periodicity on perfect Au(111) terraces exhibits extremely low friction and almost no dependence on load. Significant friction is observed only above a load threshold at which wear of the surface is initiated. In contrast, irregular stick–slip motion and a linear increase of friction with load are observed on electrochemically oxidized surfaces. The observations are discussed with reference to the amorphous structure of the oxo-hydroxide surface and atomic place exchange mechanisms upon oxidation. Reversible, fast switching between the two states of friction has been achieved in both perchloric and sulfuric acid solutions.



INTRODUCTION

Friction is a complex issue in numerous industrial applications where it leads to significant loss of energy as well as wear and tear of materials.¹ Correspondingly, the origins of friction are of fundamental scientific interest. A thorough understanding of mechanical energy dissipation requires knowledge of the materials' physical and chemical properties and study of the underlying mechanisms.² At macroscopic length scales, friction between two sliding surfaces is an average effect of numerous surface asperities shearing against each other, which makes the understanding of the exact mechanism very difficult.^{3–6} Experiments using friction force microscopy (FFM) reduce the complexity of the problem. Friction of a single asperity can be studied with nanometer or even atomic scale resolution and sub-nanonewton force sensitivity.⁷

Surface chemistry plays a crucial role for the interfacial interactions in friction experiments. High-resolution friction force microscopy experiments therefore require control of surface structure and chemistry and are carried out either in ultrahigh vacuum (UHV) or in other controlled conditions, e.g., in an electrochemical environment.^{8–13} The electrochemical environment not only allows the preparation of clean surfaces but also enables quick and reversible changes of the interface, which makes it a unique tool to investigate the effects of surface chemistry on friction. Metals are dominant materials in engineering applications involving moving contacts. They are regularly covered with an oxide layer, which makes the tribological properties of metals in their native as well as oxidized states important to address. Gold is one of the important metals due to its unique physical and chemical properties and has a growing number of

scientific and technological applications, such as in electrical contacts and electronic circuits, dental implants, medical devices, drug delivery chips, catalysis, nanosensors, and micro/nano-electromechanical systems.¹⁴ Many of these applications require knowledge of the tribological properties of gold, whose surface chemistry can be controlled at the atomic level through electrochemical methods.^{15,16}

The majority of gold oxidation studies have included the recording of cyclic voltammograms (CV) in aqueous solutions of sulfuric acid or perchloric acid. During the anodic sweep in perchloric acid solution, a broad peak is observed in the CV corresponding to the adsorption of OH ions, which subsequently leads to an oxidation when the potential is further increased.¹⁷ A place exchange of gold and oxygen atoms and the release of adsorbed anions result in an amorphous hydrous oxo-hydroxide layer, to which we will refer in short as oxidized gold surface.¹⁸ A sharper peak is observed during the cathodic potential sweep which corresponds to reduction of the gold oxide: the Au(111) atomic structure is restored below this potential with some islands and pits. The formation and structure of the oxidized gold surface have been confirmed by surface X-ray photoelectron spectroscopy¹⁹ and scattering²⁰ and scanning tunneling microscopy (STM).^{19,21–23}

Sulfate anions are specifically adsorbed on the gold surface during the anodic sweep in sulfuric acid solution and play a defined role in the oxidation process by their competition to

Received: November 11, 2010

Revised: January 16, 2011

hydroxide adsorption,^{17,24} whereas perchlorate adsorption is nonspecific in perchloric acid solution. However, the process of gold oxidation itself proceeds similarly in sulfuric and perchloric acid solutions.^{18,19}

The friction force microscopy experiments described in this paper study the role of electrochemical oxidation for the friction on gold surfaces. In an early application of atomic force microscopy in electrochemistry, Manne et al. studied the formation of hydroxide and oxide on Au(111)²⁵ as well as copper deposition on the Au(111) surface.²⁶ In their topographic studies the authors demonstrated how the electrochemically induced changes in the surface structure can be monitored on the atomic scale. Friction measurements as a function of the electrochemical potential by means of FFM have been performed by Kautek et al. at the silver halogenide interface.⁹ An increase of friction for specifically bound anions was found, while nonspecifically bound hydrated anions did not change friction. Nielinger et al. performed electrochemical FFM studies on atomically flat gold surfaces covered with a controlled thickness of copper.¹¹ They found that friction increases with the amount of copper deposited and that the increase of friction is reversible upon dissolution of the copper layers. Hausen et al. complemented these studies by showing that the increase of friction is significantly weakened by the presence of chloride.¹² Recently, Labuda et al. have extended friction studies on copper layers to the atomic scale.¹³ They confirmed that friction increases on a copper layer adsorbed by underpotential deposition on Au(111). Atomic friction maps on the copper layer reveal a structure which indicates that sliding occurs on a CuCl layer rather than on an epitaxial copper layer. All friction force microscopy studies published so far demonstrate the sensitivity of friction force microscopy to subtle electrochemically induced changes in the surface structure and chemistry.

In this article, we present a study of nanometer-scale friction of atomically flat Au(111) surfaces. Friction as a function of load for the reduced and the oxidized surface is measured by switching the potential for each load. The variation in friction as a function of the potential is investigated by recording friction while running cyclic voltammograms. The results are compared for perchloric and sulfuric acid solutions. Atomic friction results provide information about the surface structure, the lateral contact stiffness, and the surprisingly fast changes in the surface structure and in the friction upon electrochemical oxidation.

EXPERIMENTAL METHODS

Friction experiments begin by bringing the tip of the AFM, which is attached to the end of a rectangular cantilever, into contact with the gold surface. When scanning the sample, the lateral force acting on the tip causes a twisting of the cantilever, which is detected as deflection of a light beam reflected from the cantilever. The lateral force is modulated by the interaction with the surface structure. The friction force, which is proportional to the energy dissipation, is equal to the average of the measured lateral force. The averaging is done over many pairs of forward and backward scans. Note that the modulation of the lateral force is often larger than the averaged friction force and that the two do not follow a simple relationship with each other. The tip, cantilever, and sample were fully immersed in the electrolyte. The electrochemical potential was varied during the friction experiment in order to study changes in friction upon oxidation and reduction.

The experiments were performed with a home-built¹³ and a commercial (Agilent 5500) atomic force microscope. Both microscopes are capable of performing friction measurements in electrochemical

environments with high spatial and force resolution. The home-built microscope has several features which make it particularly suitable for atomic-scale friction studies. The mechanical noise is minimized by decoupling the detection components from the mechanical assembly joining the sample and cantilever, the signal amplification is optimized for small lateral force signals, and a small scan range was chosen to improve the lateral resolution.

The Au(111) substrates for the home-built AFM were thin films evaporated on a smooth sapphire surface; for sample preparations details see ref 13. Using the Agilent AFM, we studied the (111) surface of a gold single crystal (Mateck, Germany), which was prepared by annealing in a butane flame for 1 min and cooling under dry argon flow, prior to each experiment. All potentials in this article are quoted with respect to a Ag/AgCl leak-free electrode (Cypress Systems and WPI).

Friction experiments were performed using doped silicon cantilevers (nanosensors, PPP-CONT) with nominal normal and lateral stiffness values of ~ 0.1 and 40 N/m. A stiffness calibration was performed for each cantilever using Sader's method;^{27,28} the tip height was determined by scanning electron microscopy. Zero normal tip-sample force was defined as zero cantilever deflection.

In order to study the effects of surface chemistry on friction, it is necessary to exclude the influence of surface topography on the friction measurements. It is therefore imperative to work on atomically flat substrates. In perchloric and sulfuric acid solution, redox cycling causes corrosion pitting of the Au(111) surface which roughens it on the scale of several atomic layers within a few cycles.²³ Trace amounts of chloride (10^{-5} M) prevent this problem by increasing the surface mobility of gold atoms.^{23,29} The time for the recovery of atomically flat Au(111) terraces is reduced significantly,²³ allowing fast switching between atomically flat Au(111) and oxidized surfaces during the experiments.

RESULTS AND DISCUSSION

The relation between electrochemical potential, gold surface structure, and friction has been studied in solutions of perchloric acid and sulfuric acid. We will first discuss the experimental results in detail for perchloric acid, followed by a comparison to the sulfuric acid case.

Figure 1 describes the friction measured on a Au(111) surface while recording a cyclic voltammogram between 0.25 and 1.15 V, i.e., starting from a Au(111) surface, developing an oxidized gold surface, and then returning to Au(111). The lateral force map in Figure 1a initially shows smooth sliding at a low friction level. The onset of a regular modulation of the lateral force can be observed at a potential of 0.35 V. Above a potential of about 0.6 V the modulation becomes blurry. At a potential just above 0.8 V we observe a sudden and significant increase in lateral force and rather irregular patterns, which continue for all potentials up to 1.15 V. In the same range we observe increasing oxidation currents. Upon reducing the potential, low lateral forces and smooth sliding are reestablished at a potential of 0.8 V, just after passing the reduction peak in the current. Again, a period of modulation of lateral forces is observed for potentials around 0.5 V. The inset in Figure 1c reveals that in these periods the lateral force is modulated in a sawtooth-like shape with the periodicity of the Au(111) lattice.

The observed changes in the lateral force patterns occur at potentials whose significance has been described in the literature. The force modulations with atomic periodicity start at the potential of zero charge of 0.33 V.³⁰ While we cannot draw an exact picture of the tip-sample interaction in the acid solution, we conclude that the formation of the double layer plays an important role in the atomic contrast formation in friction force

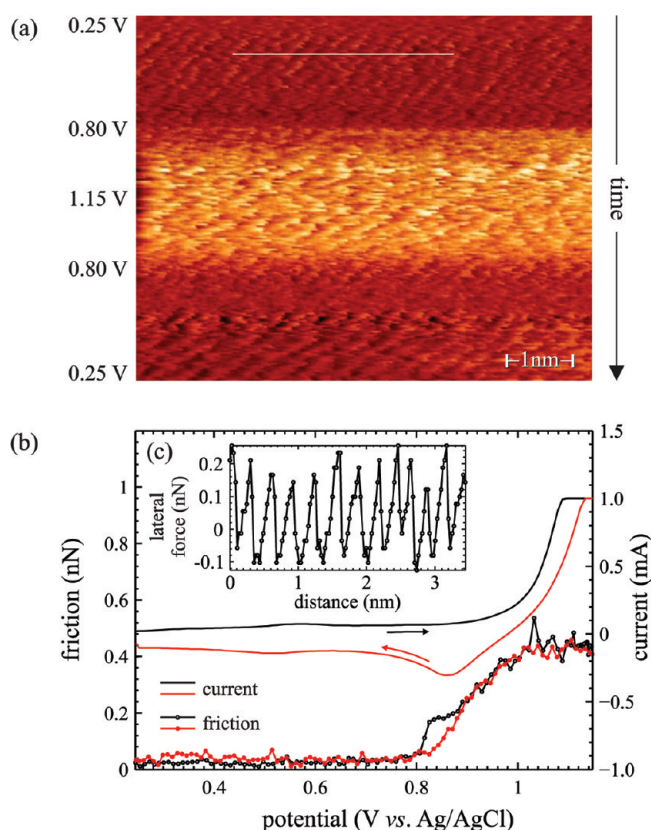


Figure 1. (a) Lateral force map recorded with the Agilent AFM on a Au(111) surface at a normal load of 6.5 nN in 0.1 M HClO₄ solution (no HCl present) while sweeping the potential continuously between 0.25 and 1.15 V and back at a rate of 25 mV/s. The slow scan direction is from top to bottom. See text for a description of frame segments with atomic stick–slip and with high friction. (b) Friction force as a function of the electrochemical potential extracted from the data shown in (a). The corresponding CV is shown in order to directly relate friction in different states to Au oxidation and reduction. (c) Cross section of the lateral force along the line indicated in (a). Atomic stick–slip with the periodicity of the Au(111) lattice is observed.

microscopy. The strong increase of the lateral force and the onset of irregular stick–slip patterns start just below the potential for hydroxide adsorption, the first step of gold surface oxidation.^{17,19,23}

Friction data are plotted together with the cyclic voltammogram in Figure 1b. Friction on the Au(111) surface is very low with values around 20 pN and independent of the electrochemical potential. Not even for potentials between 0.35 and 0.6 V, where the lateral force exhibits the atomic periodicity modulation, does friction, i.e., the average lateral force, increase. These observations confirm the report of Kautek et al., who also found no change in friction as a function of potential as long as there was no specific adsorption of anions.⁹ Specific adsorption is not expected for perchlorate ions on Au(111). Any electrostatic contributions to the forces between tip and sample, which could change with the electrochemical potential and influence the friction, are screened by the electrolyte.

Starting at a potential just above 0.8 V, i.e., a little below the usually observed potential for hydroxide adsorption, friction increases and reaches a level of about 0.4 nN at a potential of 1.0 V and higher. In this regime of high friction the data exhibit

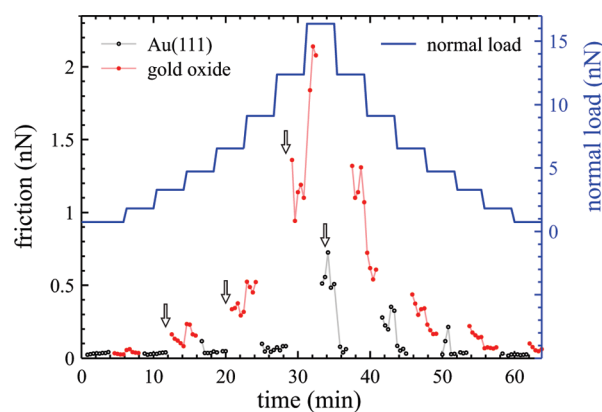


Figure 2. Time series of friction vs load measurements performed with the home-built AFM in 0.1 M HClO₄ solution, in the presence of 10^{−5} M HCl. The normal force was increased and decreased in steps, while for each load the friction was measured on Au(111) and oxidized surfaces, by switching the potential between 0.5 and 1.4 V. Each data point represents the average friction of one lateral force map of 10 nm, and each frame was recorded in 25 s. The arrows refer to atomic friction maps in Figure 4.

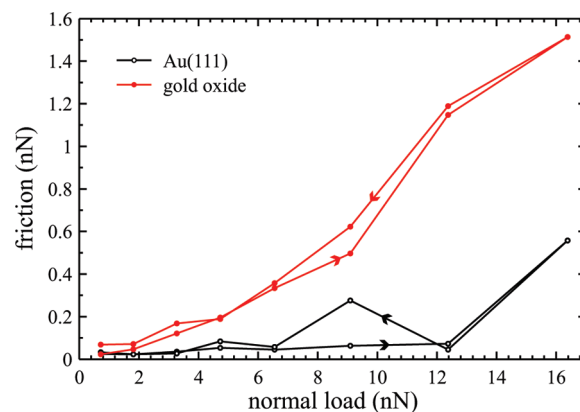


Figure 3. Friction vs load results for Au(111) and oxidized surfaces recorded in 0.1 M HClO₄ solution, in the presence of 10^{−5} M HCl. The graph summarizes the results of the experiment in Figure 2.

some scatter consistent with the rather irregular stick–slip behavior of the sliding interface. As introduced above, the oxidation process of gold surfaces has been described as a hydroxide adsorption into a surface network followed by a place exchange of gold and oxygen species and further oxidation.¹⁸ The irregular stick–slip and the scatter in the friction data can be understood in view of this continuing turnover of the surface structure. In the cathodic scan, friction starts to decrease around a potential of 1.0 V when the reduction peak is observed in the current. Friction reaches the low level of 20 pN again around 0.8 V. A fast recovery of the Au(111) surface upon reduction without pitting is observed even without added chloride in cases where the oxidation did not exceed far beyond the principal oxidation peak at 1.25 V, as previously reported in a STM study.²³

A key experiment in friction studies is the measurement of friction as a function of the applied load. A linear dependence is regularly found from macroscopic to microscopic scales in weakly adhesive situations like the one studied here.³¹ We have recorded friction as a function of applied load, while switching

between the reduced and the oxidized Au surface for each value of applied load. In this way we could exclude that a change in the tip structure obscures the load dependence of friction for both surfaces. Results for this experiment are plotted in chronological order in Figure 2. Each point in this graph represents the average friction of a lateral force map. Load and potential have been switched in between frames. The scatter between data points recorded in equivalent conditions is not caused by instrumental noise, but by minor changes in the atomic structure of the tip–sample contact. Note that the scatter is small compared to the friction contrast caused by changes in load and potential.

The first and most important observation is that friction increases with load significantly only for the oxidized surface, while it remains at low values for the reduced Au(111) surface. This result is summarized in Figure 3 where friction is plotted as a function of load for both surfaces. While there is almost no increase in friction for Au(111), the oxidized surface exhibits the expected linear increase with load. Only at loads higher than 12 nN do we find significant friction on Au(111) with a large scatter of corresponding data points in Figure 2. These observations indicate the onset of wear for loads higher than 12 nN, i.e., a destruction of the Au(111) surface by the scanning tip. Very similar observations of extremely low friction at low loads and increased friction at the onset of wear have been made in friction measurements on Au(111) in ultrahigh vacuum.³² We conclude that friction is extremely low and almost independent of load as long as the tip slides over a perfect crystalline Au(111) surface. Significant friction is observed only when the load is high enough to displace surface atoms.

These conclusions are supported by atomic-scale lateral force maps recorded during the experiment depicted in Figure 2. The lateral force recorded on the reduced Au(111) surfaces exhibits a periodic modulation which reflects the crystalline structure of the Au(111) surface. Examples for atomic friction maps of Au(111) are given in the upper halves of the frames in Figure 4. Scanning at constant potential and use of dedicated instrumentation¹³ allows for high-quality lateral force data. Line profiles of the lateral force have a sawtooth profile indicative of an atomic stick–slip process: the contact sticks to one atomically locked position until the lateral force is high enough to initiate a jump to the next atomic position. While the contact between tip and surface is not formed by a single atom but may consist of some tens of atoms, the atomic structure of the surface is still revealed in atomic friction experiments. The atomic slipping may actually occur as a simultaneous jump of all atoms in contact or as fast propagation of a dislocation through the contact.⁶ Similar atomic stick–slip results have been reported for experiments on clean metal surfaces in ultrahigh-vacuum environments.^{32–34}

Oxidation of the surface immediately eliminates the atomic periodicity of the stick–slip mechanism. This is demonstrated in Figure 4, where the potential is switched after half a lateral force map is recorded. The regular hexagonal stick–slip pattern is replaced by a stick–slip pattern which still shows nanometer-scale features, however irregularly arranged. We conclude that the stick–slip mechanism works not only on single-crystal surfaces but also on the disordered surface after hydroxide adsorption. Irregular stick–slip on the nanometer scale agrees well with the observation of arrays of small clusters 1–2 nm in average size by STM at the onset of electrochemical oxidation.¹⁹ At higher loads the lateral force maps recorded on the oxidized surface show stripes along the scan direction which indicate displacement of surface atoms or clusters by the action of the tip.

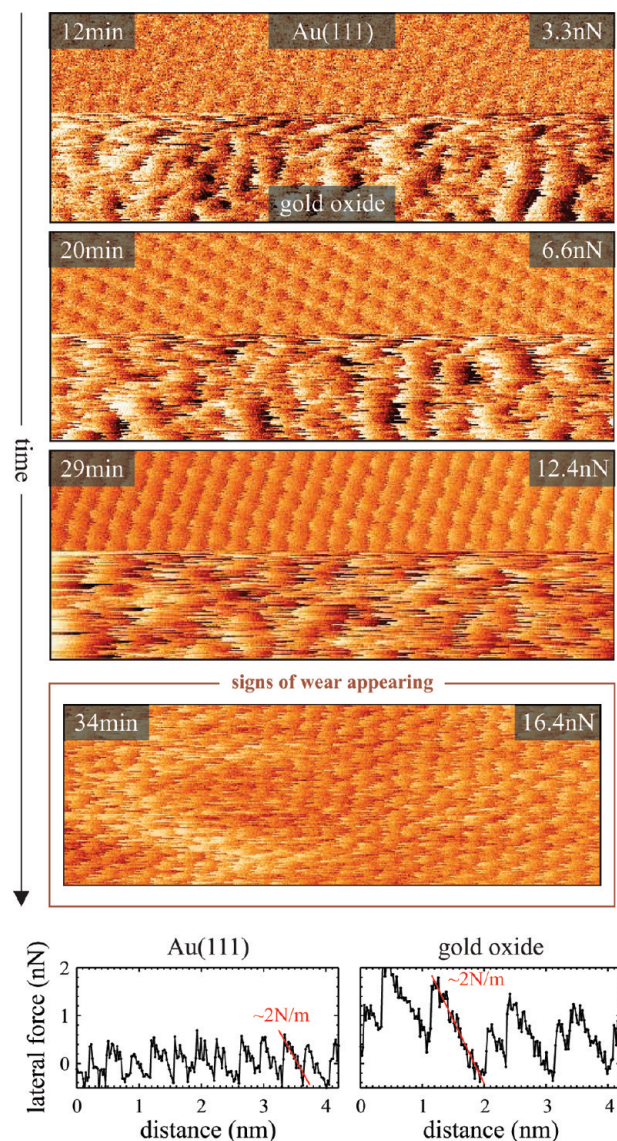


Figure 4. Examples for lateral force maps of the transition from Au(111) to the oxidized surface recorded with the home-built AFM in 0.1 M HClO₄, in the presence of 10^{−5} M HCl. Scan direction is from top to down. In the three upper frames, the potential is switched from 0.5 to 1.4 V after the half of the frame is scanned. Times and forces indicated refer to the time and load in the experiment depicted in Figure 2. The lateral force is modulated by stick–slip motion on both surfaces, revealing atomic periodicity on the crystalline Au(111) surface in the upper half and nonperiodic events on the amorphous oxidized surface in the lower half. The fourth frame shows signs of wear on the reduced Au(111) surface at higher load. The cross sections of the lateral force are taken from the data recorded at a load of 12.4 nN. The red lines indicate the effective lateral contact stiffness.

While the nanometer-scale features can be recognized in consecutive scan lines, the overall structure is not reproduced in consecutive scan frames. Given the dynamic rearrangement of the surface during oxidation, such atomic instabilities are to be expected. The stress caused by the sliding tip may actually accelerate the oxidation process, which is otherwise hindered by the necessity of an atomic place exchange.¹⁸ The atomic friction results relate the threshold for friction on the perfect Au(111) surface (around 12 nN in the example in Figure 3) to

the visible onset of wear. They furthermore relate the increase of friction with load on oxidized surfaces to the displacement of surface atoms which is found increasingly at all loads on the amorphous oxo-hydroxide surface.

The transition from low friction on Au(111) to irregular stick–slip and high friction on the oxidized surface occurs instantaneously on the time-scale of our measurements (<100 ms), as observed in the sharpness of the respective transitions in Figure 4. While adsorption of hydroxide on Au(111) may generally happen at the millisecond time scale,¹⁸ we consider it noteworthy that the confinement of the solution under the AFM tip does not cause any delay of the switching. The transition back from the oxidized surface to the Au(111) surface occurs within seconds. We observe signs of an atomic rearrangement which was not reproducible in its details between experiments. However, the friction drops to its low value in less than 1 s, and the hexagonal stick–slip pattern is reestablished within a few seconds. The switching of friction by changing the potential is reversible and repeatedly reproducible for at least 100 cycles. Traces of chloride are required for repeated switching, as discussed at the end of the Experimental Methods section.

The slope of the sawtooth stick–slip curves in Figure 4 quantifies the effective lateral stiffness of the contact between tip and surface. Typical values for Au(111) are 2 N/m with a significant scatter of ± 0.5 N/m due to the noisy character of the data. The effective stiffness is much smaller than the spring constant for the cantilever torsion and, therefore, reflects the lateral stiffness of the contact rather than that of the cantilever. The values are of the same order than in results obtained on Au(111) in ultrahigh-vacuum conditions.³² The lateral contact stiffness is a measure of the stiffness of the tip apex and of the contact size.³⁵ For the oxidized gold surface the values for the effective lateral contact stiffness extracted from stick–slip curves are the same as for Au(111) within error. We conclude that the contact size does not change significantly upon oxidation of the surface. The increase in friction must originate in other factors which change upon oxidation. One factor is certainly the increased roughness of the oxidized surface, which strengthens the resistance against sliding of the amorphous tip. Another factor may be the irregular charge distribution of the oxidized Au surface, introduced above as an amorphous oxo-hydroxide layer. Local dipoles should interact more strongly with the silicon oxide tip, charged at pH < 2, than the metallic Au(111) surface. Finally, energy may be dissipated in tip-induced changes of the atomic configuration of the oxidized layer, which do not take place on the crystalline Au(111) surface.

Finally, we compare experiments regarding the load dependence of friction on Au(111) and the oxidized surface in perchloric and sulfuric acid. Results for sulfuric acid are plotted in Figure 5. Again friction was measured at each applied load for Au(111) and the oxidized surface. Very similar to the results for perchloric acid, friction increases significantly only for the oxidized gold surface. The corresponding friction vs load curve is given in Figure 6. The similarity of the results for both solutions agrees well with STM studies that found no significant difference in the electrochemical oxidation of Au(111) between perchloric acid and sulfuric acid.¹⁹ Once the electroadsorption of hydroxide has displaced the specific adsorption of sulfate, possibly pre-adsorbed chloride, or the nonspecific adsorption of perchlorate, no further difference in the oxidation process is expected between the two solutions.¹⁸ Possible subtle differences in friction in the anion adsorption regime are subject of ongoing

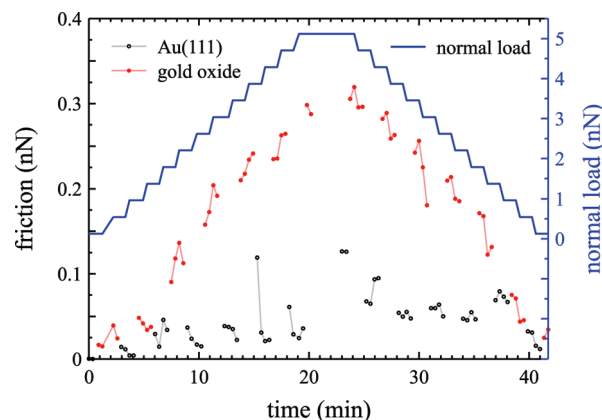


Figure 5. Time series of the friction vs load measurements performed with the Agilent AFM in 0.05 M H₂SO₄ + 1 mM HCl solution. The normal force was increased and decreased in steps, while for each load the friction was measured on Au(111) and oxidized surfaces, by switching the potential between 0.35 and 1.0 V.

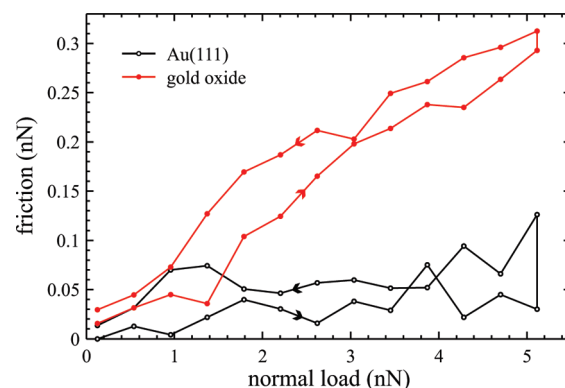


Figure 6. Friction vs load results for Au(111) and oxidized surfaces in 0.05 M H₂SO₄ + 1 mM HCl solution. The graph summarizes the results of the experiment in Figure 5.

experiments. Our results confirm that friction on the oxidized Au surface does not significantly differ between perchloric and sulfuric acid solutions and their specific oxidation processes.

CONCLUSION

A strong contrast in friction between reduced and oxidized Au surfaces at the nanometer scale has been observed reproducibly in two laboratories with different instrumentation and for sulfuric and perchloric acid solutions. Extremely low friction and almost no increase with load are found for sliding on perfect crystalline Au(111) surfaces. Modulation of the lateral force in a sawtooth fashion reveals an atomic stick–slip sliding mechanism. Only above a certain load threshold does friction increase; this corresponds to the onset of surface wear.

On the oxidized Au surface, friction increases with load as generally expected. An irregular stick–slip motion reflects the amorphous structure of the oxo-hydroxide surface and the displacement of surface atoms even at low loads. Fast, reversible switching between the two states of friction is achieved by electrochemical control.

AUTHOR INFORMATION

Corresponding Author

*E-mail: roland.bennewitz@inm-gmbh.de.

ACKNOWLEDGMENT

The authors are thankful for research funding from the Canada Foundation for Innovation (CFI), the Natural Research and Engineering Research Council (NSERC), and the Alexander von Humboldt foundation. Co-authors at the INM thank Eduard Arzt for continuing support and fruitful discussions.

REFERENCES

- (1) Jones, M.; Scott, D. *Industrial Tribology: The Practical Aspects of Friction, Lubrication, and Wear*; Elsevier: Dordrecht, The Netherlands, 1983.
- (2) Buckley, D. H. *Surface Effects in Adhesion, Friction, Wear and Lubrication*; Elsevier: New York, 1986.
- (3) Persson, B. *Sliding Friction*, 2nd ed.; NanoScience and Technology; Springer: Berlin, 2000.
- (4) Bowden, F.; Tabor, D. *The Friction and Lubrication of Solids*; Clarendon: Oxford, 1986.
- (5) Rabinowicz, E. *Friction and Wear of Materials*; John Wiley: New York, 1995.
- (6) Merkle, A. P.; Marks, L. D. *Tribol. Lett.* **2007**, *26*, 73–84.
- (7) Meyer, E.; Overney, R.; Dransfeld, K.; Gyalog, T. *Nanoscience: Friction and Rheology on the Nanometer Scale*; World Scientific: Singapore, 1998.
- (8) Binggeli, M.; Christoph, R.; Hintermann, H.; Marti, O. *Surf. Coat. Technol.* **1993**, *62*, 523–528.
- (9) Kautek, W.; Dieluweit, S.; Sahre, M. *J. Phys. Chem. B* **1997**, *101*, 2709–2715.
- (10) Schnyder, B.; Alliata, D.; Kotz, R.; Siegenthaler, H. *Appl. Surf. Sci.* **2001**, *173*, 221–232.
- (11) Nielinger, M.; Baltruschat, H. *Phys. Chem. Chem. Phys.* **2007**, *9*, 3965–3969.
- (12) Hausen, F.; Nielinger, M.; Ernst, S.; Baltruschat, H. *Electrochim. Acta* **2008**, *53*, 6058–6063.
- (13) Labuda, A.; Paul, W.; Pietrobon, B.; Lennox, R.; Grütter, P.; Bennewitz, R. *Rev. Sci. Instrum.* **2010**, *81*, 083701.
- (14) Corti, C.; Holliday, R. *Gold: Science and Applications*; CRC Press: London, 2010.
- (15) Gewirth, A. A.; Niece, B. K. *Chem. Rev.* **1997**, *97*, 1129–1162.
- (16) Herrero, E.; Buller, L. J.; Abruna, H. D. *Chem. Rev.* **2001**, *101*, 1897–1930.
- (17) Angerstein-Kozłowska, H.; Conway, B.; Hamelin, A.; Stoicoviciu, L. *J. Electroanal. Chem.* **1987**, *228*, 429–453.
- (18) Conway, B. *Prog. Surf. Sci.* **1995**, *49*, 331–452.
- (19) Rodriguez Nieto, F. J.; Andreasen, G.; Martins, M. E.; Castez, F.; Salvezza, R. C.; Arvia, A. J. *J. Phys. Chem. B* **2003**, *107*, 11452–11466.
- (20) Kondo, T.; Morita, J.; Hanaoka, K.; Takakusagi, S.; Tamura, K.; Takahashi, M.; Mizuki, J.; Uosaki, K. *J. Phys. Chem. C* **2007**, *111*, 13197–13204.
- (21) Gao, X.; Weaver, M. *J. Electroanal. Chem.* **1994**, *367*, 259–264.
- (22) Schneeweiss, M.; Kolb, D. *Solid State Ionics* **1997**, *94*, 171–179.
- (23) Trevor, D. J.; Chidsey, C. E. D.; Loiacono, D. N. *Phys. Rev. Lett.* **1989**, *62*, 929–932.
- (24) Angerstein-Kozłowska, H.; Conway, B. E.; Hamelin, A.; Stoicoviciu, L. *Electrochim. Acta* **1986**, *31*, 1051–1061.
- (25) Manne, S.; Massie, J.; Elings, V. B.; Hansma, P. K.; Gewirth, A. A. *J. Vac. Sci. Technol. B* **1991**, *9*, 950–954.
- (26) Manne, S.; Hansma, P. K.; Massie, J.; Elings, V.; Gewirth, A. A. *Science* **1991**, *251*, 183–186.
- (27) Green, C.; Lioe, J.; Cleveland, H.; Proksch, R.; Mulvaney, P.; Sader, J. *Rev. Sci. Instrum.* **2004**, *75*, 1988–96.
- (28) Sader, J. *Rev. Sci. Instrum.* **1999**, *70*, 3967.
- (29) Cahan, B.; Villullas, H.; Yeager, E. *J. Electroanal. Chem.* **1991**, *306*, 213–238.
- (30) Hamm, U.; Kramer, D.; Zhai, R.; Kolb, D. *J. Electroanal. Chem.* **1996**, *414*, 85–89.
- (31) Gao, J.; Luedtke, W.; Gourdon, D.; Ruths, M.; Israelachvili, J.; Landman, U. *J. Phys. Chem. B* **2004**, *108*, 3410–3425.
- (32) Gosvami, N. N.; Filleter, T.; Egberts, P.; Bennewitz, R. *Tribol. Lett.* **2010**, *39*, 19–24.
- (33) Bennewitz, R.; Gnecco, E.; Gyalog, T.; Meyer, E. *Tribol. Lett.* **2001**, *10*, 51.
- (34) Enachescu, M.; Carpick, R.; Ogletree, D.; Salmeron, M. *J. Appl. Phys.* **2004**, *95*, 7694–7700.
- (35) Carpick, R.; Ogletree, D.; Salmeron, M. *J. Appl. Phys. Lett.* **1997**, *70*, 1548.